Contents lists available at ScienceDirect

Advances in Colloid and Interface Science

journal homepage: www.elsevier.com/locate/cis

Aggregation in colloidal suspensions: Effect of colloidal forces and hydrodynamic interactions

N.M. Kovalchuk [a,b], V.M. Starov [c,*]

[a] Institute of Biocolloid Chemistry, 03142 Kiev, Ukraine
[b] Max-Planck Institute of Colloids and Interfaces, D-14424 Potsdam/Golm, Germany
[c] Department of Chemical Engineering, Loughborough University, LE11 3TU Loughborough, UK

ABSTRACT

The forces acting in colloidal suspensions and affecting their stability and aggregation kinetics are considered. The approximations used for these forces in numerical simulations and the importance of the balanced account for both colloidal forces and hydrodynamic interactions are discussed. As an example the results of direct numerical simulations of kinetics of aggregation either with account for hydrodynamic interaction between particles or without it are compared by varying the parameters of the interaction potential between particles and fraction of solid. Simulations are based on the Langevin equations with pairwise interaction between particles and take into account Brownian, hydrodynamic and colloidal forces. It is confirmed that the neglecting of hydrodynamic interaction results in an accelerated growth of aggregates. The results of numerical simulations of aggregation kinetics are compared with well known analytical solutions.

© 2011 Elsevier B.V. Open access under CC BY license.

1. Introduction

Aggregation in colloidal dispersions, suspensions and emulsions, is important for many natural phenomena and industrial processes. Stability in these systems is determined by the relation of attractive and repulsive forces acting between particles [1–3]. If attractive forces (van der Waals forces or/and depletion interaction in the dispersion medium containing a non-adsorbing polymer) prevail, particles coagulate irreversibly in the deep primary potential well, forming large aggregate with fractal structure, characterized by the power law dependency of mass of the aggregate M on the radius of gyration R_g [4–6]:

where $1 < d_f < 3$ is the mass fractal dimension. In the absence of long-range repulsive forces the aggregation kinetics is diffusion limited (DLCA) [7] with typical value of the mass fractal dimension about 1.8.

If the repulsion is included, for example, due to electrical charge on particle surfaces or adsorbed on their surface polymer, then potential barrier appears complicating aggregation. In the latter case not each collision of two particles results in their aggregation. Aggregation slows down being reaction limited (RLCA) [8]. Particles have more time for the rearrangement inside the aggregate, therefore RLCA results in formation of denser aggregates in comparison with DLCA,

with the mass fractal dimension about 2.1. The probability of sticking decreases with the increase of the height of the potential barrier and when repulsion is strong enough, dispersion becomes kinetically stable, i.e. particles do not aggregate during a long period of time.

In the presence of both, attraction and repulsion, between particles a colloidal dispersion can reveal a more complicated behavior than the only either kinetic stability or irreversible coagulation. The reversible coagulation in the relatively shallow secondary potential well [9,10] can result in formation of aggregates of finite size in dynamic equilibrium with singlets, especially when the potential barrier between primary and secondary potential well is high enough to prevent the jumping of particles into the primary potential well. The average size of aggregates is determined by the dynamic equilibrium ___ ___ ___ ___ween particles and ___ ___ ___ and should therefore ___ ___ ___ ___ al well. If the latter is large enough, then the irreversible aggregation with an unlimited growth of aggregates occurs even in the secondary potential well [11]. It has been assumed, that there can be also other mechanisms resulting in the formation of stable aggregates of colloidal particles, which stop to grow after reaching a certain size, when the long range repulsion between colloidal particles compete with attraction [12–14]. Formation of phase of stable clusters in equilibrium with singlets has been observed in many investigations [15–23] employing different experimental techniques, including direct observations by confocal microscopy [19–22].

The clear understanding and correct prediction of aggregation kinetics and mechanisms responsible for formation of stable aggregates as well as estimation of equilibrium size of aggregates on the

* Corresponding author.
  E-mail address: V.M.Starov@lboro.ac.uk (V.M. Starov).

basis of properties of dispersed particles and dispersion medium is of great importance, as aggregation can change drastically the physical properties of colloidal dispersion, in particular its rheology [24–29].

Below the forces coming into play in colloidal dispersions and determining either their stability or aggregation kinetics are reviewed together with suitable approximations of these forces used in numerical simulations. The attention is paid to aggregation in the relatively shallow potential well, with depth of up to 20 kT. Some original results of numerical simulations are used along with published data to illustrate the effect of fraction of solid, potential well characteristics and hydrodynamic interactions on aggregation kinetics and equilibrium aggregates size in the case of reversible aggregation.

2. Numerical modelling and representation of forces acting in colloidal suspensions

One of the most powerful tools to study aggregation processes in colloidal suspensions is numerical simulations. There are a number of simulation methods developed, enabling simulations of kinetics and/or equilibrium properties. Well known examples are Monte–Karlo [30–32], molecular dynamic [13,33] and their modifications, dissipative particles dynamic simulations [34] as well as numerical solution of population balance equations [35–38]. Below we focus on another widely used method which is highly suitable for studying of aggregation kinetics, the Brownian dynamic simulations [39–42]. The latter method is based on the numerical solution of Langevin equations [43–46]. This method enables a direct simulation of time evolution of ensemble of particles immersed in a dispersion medium considered as a structureless continuum with a defined viscosity. The review of Monte–Karlo, molecular dynamics and Brownian dynamics modeling techniques is given for example in [47,48].

The crucial step in the Brownian dynamic simulations is a proper choice of forces acting on particles and between particles. On the one hand, a certain simplification of model is required to get the reasonable simulations time, but on the other hand, the model has to retain the essential physics of real systems. The DLVO theory [1–3] provides a good basis for description of colloidal forces between particles. Usually particles are considered as being identical and spherical and forces between them pairwise additive. Most commonly the London–van der Waals dispersion forces are used for attraction [24,49–51]:

$$U_{VdW} = -\frac{A}{6}\left[\frac{2a^2}{h(4a+h)} + \frac{2a^2}{(2a+h)^2} + \ln\frac{h(4a+h)}{(2a+h)^2}\right], \quad (2)$$

where A is Hamaker constant, a is the particle radius, h is the surface to surface separation between particles, and electrostatic double layer interaction for repulsion [24,49–51]:

$$U_{DL} = 2\pi\varepsilon\psi_0^2 a \frac{2a}{2a+h} \exp(-\kappa h) \qquad \kappa a < 5, \quad (3)$$

$$U_{DL} = 2\pi\varepsilon\psi_0^2 a \ln\{1 + \exp(-\kappa h)\} \qquad \kappa a > 5, \quad (4)$$

where $\varepsilon = \varepsilon_0\varepsilon_r$ is the permittivity of the medium, ε_0 is the permittivity of vacuum and ε_r is the relative permittivity or dielectric constant, ψ_0 is the surface potential of particles, κ^{-1} is the Debye screening length. For z–z electrolyte

$$\kappa = \left(\frac{\varepsilon kT}{2z^2 e^2 n_b}\right)^{-1/2}, \quad (5)$$

where k is the Boltzman constant, T is the temperature and n_b is the number density of ions in the bulk.

Here the aggregation of colloidal particles in the relatively shallow potential well is of the main interest, in particular, aggregation in the secondary potential well. The usual distance of the secondary potential well to the interface is of the order of 10–100 nm [52]. That means that by rigorous consideration of the problem the retardation of dispersion forces should be taken into account. The comprehensive discussion on retardation problem is given in [47,52]. Retardation means that the Hamaker constant A in Eq. (2) in reality is not a constant, but decreases with the increase of the distance to the surface of a particle. For example, according to the results of numerical simulations [53] the value of Hamaker constant for gold in water decreases about twice by the increase of separation from 1 to 20 nm. The values of Hamaker constant given in reference books are those for small separations, where retardation is negligible. Therefore, by using them the depth of the secondary potential well is overestimated, as shown in Ref [52], Fig. 1.15.

Other forces which can come into play are as follows. Depletion attraction due to presence of non-adsorbing polymer [54] (or nano-particles) can be calculated as [24]:

$$U_D = -\frac{4\pi}{3}(a+\delta)^3\left(1 - \frac{3(2a+h)}{4(a+\delta)} + \frac{(2a+h)^3}{16(a+\delta)^3}\right)\Pi \quad \text{at } h < 2\delta,$$

$$U_D = 0 \text{ at } h > 2\delta, \quad (6)$$

where δ is the equivalent-hard sphere radius of depleting species, Π is the osmotic pressure in the bulk. For ideal solutions $\Pi = \rho kT$, where ρ is the number density of macromolecules. However, if non-ideality of the polymer solution is taken into account then:

$$\Pi = \rho kT\left(1 + \frac{2nM}{\rho_m N_A}\right), \quad (7)$$

where N_A is the Avogadro number, M is the mean molecular weight of polymer and ρ_m its mass density, n is number density.

The repulsive hydration energy U_H [1,24,55]:

$$U_H(h) = \pi a\lambda^2 P_0 \exp(-h/\lambda), \quad (8)$$

where λ is the decay length (usually in the range 0.2–1.1 nm for 1:1 electrolytes), and P_0 is the hydration pressure constant, which increases with materials' hydrophilicity.

The energy of structural repulsion in the case of particles covered by polymer can be estimated as [2,24]:

$$U_p(h) = kT\frac{100aL^2}{\pi s^3} \exp(-\pi h/L), \quad (9)$$

where L is the thickness of attached polymer chains, s is the average distance between the chain attachment points at the surface of particle.

The particles can encounter each other because they move with different velocities in the dispersion medium. Here we consider the case without any imposed flow. The small particles are then in random Brownian motion and aggregation is called perikinetic. When the particles size is large enough the gravitation should be taken into account. In a polydisperse suspension large particles move with different velocities depending on their size (differential sedimentation) and aggregation is called orthokinetic. The effect of gravity on the aggregation of suspensions is discussed in details in Ref. [56]. The relative importance of Brownian motion and sedimentation is determined by the Peclet number:

$$Pe = \frac{2\pi\Delta\rho ga^4}{3kT}, \quad (10)$$

where $\Delta\rho$ is the density difference between dispersed material and dispersion medium, g is the acceleration due to gravity. When $Pe \ll 1$ Brownian motion dominates and aggregation is pure perikinetic, whereas at $Pe \gg 1$ aggregation is mainly orthokinetic, due to differential sedimentation. By taking $Pe = 1$ the critical diameter of particles can be estimated as about 1–3 mkm depending on $\Delta\rho$.

If aggregation occurs in the secondary potential well, particles can jump over the barrier into primary potential well [57,58]. In this case all particles eventually will be aggregated irreversibly. Only if a potential barrier is high enough aggregation can be considered as a reversible.

It is obvious that Eqs. (2)–(9) are rather complicated and their direct implementation into numerical schemes will result in the considerable increase of computational time. That is why simplified representations of interaction potentials are often used, such, for example, as Lennard–Jones potential describing attraction and steric repulsion [13,14,48]:

$$U_{LJ}(h) = 4\varepsilon_{LJ}\left[\left(\frac{a}{h+a}\right)^{12} - \left(\frac{a}{h+a}\right)^{6}\right], \tag{11}$$

where ε_{LJ} is the characteristic potential energy minimum; or Yukawa potential for a long-ranged repulsion [13,14]:

$$U_Y(h) = A_Y\frac{e^{-(h+a)/\xi}}{(h+a)/\xi}, \tag{12}$$

where A_Y and ξ are parameters.

However, the combination of potentials (11) and (12) does not produce the secondary potential minimum [14], which is of interest below.

Sometimes for a simplification the colloidal forces are omitted at all, but replaced by an approximation of sticky particles, aggregated irreversibly when interparticle separation becomes smaller than certain arbitrary chosen value, i.e. approximation of square potential well of infinite depth [59]. It seems, however, that such approximation is too rough, especially for kinetic studies, because particles begin to feel each other only at the moment, when they stick together.

Much more promising approximation for colloidal forces has been used in [60,61], where colloidal forces $F(h)$ were modelled instead of interaction energy as:

$$F(h) = C\frac{(h-h_1)(h-h_2)(h-h_3)}{h^5}, \tag{13}$$

where h_1, h_2, h_3 are positions where the force is equal to zero; C is a constant depending on the particles sizes and physicochemical properties of components of dispersion. The colloidal forces modeled in such way are similar to the real colloidal interaction forces having three intersection points with abscissa axis corresponding to equilibrium positions. A similar approach is used in the presented study enabling to investigate the dependence of aggregation kinetics not only on the depth of potential well, but also on the shape of the energy curve.

The conservative forces acting between particles are not only ones affecting the kinetics of aggregation. It has been shown [48,62,63], that hydrodynamic interactions between particles slow down the aggregation, i.e. a reasonable approximation for hydrodynamic interaction is vital for the adequate description of aggregation kinetics. Unfortunately, calculation of the full tensor of hydrodynamic friction coefficients or mobility tensor, which is mainly used in the Brownian dynamic simulations is unrealistic. The elements of mobility tensor have been tabulated only for the case of two equal particles [64]. That is why in many numerical studies the hydrodynamic interactions are neglected at all and hydrodynamic resistance to the particle motion is assumed to be constant and independent of presence of other particles [59,65,66]. The comparison of simulation results for two interacting particles using either mobility tensor proposed in [63] or Oseen approximation has shown that at close separation the Oseen tensor overestimates greatly the tendency of two spheres to move towards each other [67].

A good compromise has been proposed in [68], where it has been shown that a mobility tensor calculated by taking into account the hydrodynamic interactions between nearest neighbors in the lubrications approximation, assuming pairwise additivity of these interactions retains the essential physics of aggregation process. This approach was developed further in [69,70] employing in the numerical scheme calculation of the hydrodynamic resistance coefficients instead of mobility tensor. This enabled to avoid the matrix inversion. Below, as an example, the mathematical model and numerical scheme developed in [69,70] is used to study the effect of fraction of solid, colloidal forces and hydrodynamic interactions on kinetics of aggregation in colloidal suspensions.

3. Mathematical model

The detailed description of the model is given elsewhere [69,70] therefore below are presented the only main points. We consider 2D suspension composed of N identical particles in a Newtonian dispersion medium. The motion of each particle is governed by Langevin equation [43–46]:

$$m\frac{dV_i}{dt} = -\sum_{j=1}^{2N}\varsigma_{ij}V_j + \sum_{j=1}^{2N}\alpha_{ij}f_j + \sum_{j=1}^{2N}F_{ij}, \tag{14}$$

where $i,j = 1\ldots2$ N, $m = \frac{4}{3}\pi a^3(\rho_p + 0.5\rho_l)$ is the mass of the particle (including the added mass), ρ_p is the density of the particle material, ρ_l is the density of the suspending liquid, V is the particle velocity, ς_{ij} is the element of the hydrodynamic resistance tensor, αf represents the Brownian forces, with f_i being a random quantity, normally distributed, with

$$f_i = 0, \tag{15}$$

$$f_i(t)f_j(t') = 2\delta_{ij}\delta(t-t'), \tag{16}$$

and F represents the colloidal forces.

The matrix of hydrodynamic resistance coefficients and matrix of Brownian coefficients are correlated according to the fluctuation–dissipation theorem [39]:

$$\varsigma_{ij} = \frac{1}{kT}\sum_l \alpha_{il}\alpha_{lj}. \tag{17}$$

It is assumed below that all forces, including hydrodynamic forces, are pairwise additive, and for any pair of particles the hydrodynamic interaction depends only on the distance between them and their relative velocities.

The most important for the aggregation processes are hydrodynamic interaction at short distances between particles, where also colloidal forces come into play. To model them, the lubrication approximation derived in [71] is used for small separation between particles $h \leq 0.1a$:

$$\varsigma_x = \frac{3}{2}\pi\mu\frac{a^2}{h}, \tag{18}$$

$$\varsigma_y = \pi\mu a\ \ln\left(\frac{a}{h}\right), \tag{19}$$

where μ is the dynamic viscosity of the suspending liquid, local x axis is directed along particles center to center line, y axis in perpendicular direction. It is assumed that the hydrodynamic interaction becomes

negligible at $h > 2.5a$ and in this case ς is a scalar determined by Stokes law:

$$\varsigma = 6\pi\mu a. \tag{20}$$

The interaction forces for $0.1a \leq h \leq 2.5a$ were fitted by polynoms to enable a smooth transition over the whole hydrodynamic interaction region. Eq. (19) was also fitted by a polynom to simplify numerical procedure.

Then the matrix of hydrodynamic resistance for two interacting particles can be written as:

$$\hat{\varsigma} = \begin{pmatrix} \varsigma + \varsigma_x & 0 & -\varsigma_x & 0 \\ 0 & \varsigma + \varsigma_y & 0 & -\varsigma_y \\ -\varsigma_x & 0 & \varsigma + \varsigma_x & 0 \\ 0 & -\varsigma_y & 0 & \varsigma + \varsigma_y \end{pmatrix} \tag{21}$$

with ς_x, ς_y and ς given by Eqs. (18)–(20).

The matrix of Brownian coefficients has the same form as the matrix of hydrodynamic coefficients:

$$\hat{\alpha} = \begin{pmatrix} \alpha_{11} & 0 & \alpha_{13} & 0 \\ 0 & \alpha_{22} & 0 & \alpha_{24} \\ \alpha_{13} & 0 & \alpha_{11} & 0 \\ 0 & \alpha_{24} & 0 & \alpha_{22} \end{pmatrix}. \tag{22}$$

with

$$\begin{aligned} \alpha_{11} &= \frac{1}{2}\sqrt{kT}\left(\sqrt{\varsigma} + \sqrt{\varsigma + 2\varsigma_x}\right) \\ \alpha_{13} &= \frac{1}{2}\sqrt{kT}\left(\sqrt{\varsigma} - \sqrt{\varsigma + 2\varsigma_x}\right) \\ \alpha_{22} &= \frac{1}{2}\sqrt{kT}\left(\sqrt{\varsigma} + \sqrt{\varsigma + 2\varsigma_y}\right) \\ \alpha_{24} &= \frac{1}{2}\sqrt{kT}\left(\sqrt{\varsigma} - \sqrt{\varsigma + 2\varsigma_y}\right) \end{aligned} \tag{23}$$

The random functions f_i were modelled as [72,73]:

$$f_i = \sqrt{\frac{2}{dt}} R_{ND}, \tag{24}$$

where dt is the time step to be chosen for numerical simulations, R_{ND} is a random number from a normal distribution with mean value equal to zero and standard deviation equal to 1.

To model colloidal forces the simplified linear expression with parameters h_1, h_2, h_0 and U_{min}, corresponding to the depth of potential well, has been used for the dependency of normal force per unit area between two parallel flat surfaces, $\Pi(h)$, on distance between them:

$$\Pi = \frac{2U_{min}}{\pi a R}\frac{h_1 - h}{h_1 - h_0}, \qquad 0 < h < h_0, \tag{25a}$$

$$\Pi = \frac{2U_{min}}{\pi a R}\frac{h_2 - h}{h_2 - h_0}, \qquad h_0 < h < h_2, \tag{25b}$$

where $R = \frac{S^3}{3(h_1 - h_0)} + \frac{(h_2 - h_0)^2 - (h_1 - h_0)^2}{3} + (h_2 - h_1)(S + h_0 - h_1)$ and

$S = \sqrt{(h_0 - h_1)(h_2 - h_1)}$.

According to the Derjaguin approximation [1,2] the colloidal force acting along the centre line between particles made of the same

material as above flat surfaces and placed in the same medium is equal to

$$F(h) = \pi a \int_h^\infty \Pi(h)\,dh, \tag{26}$$

The interaction energy is:

$$U(h) = \int_h^\infty F(h)\,dh \tag{27}$$

The interaction energy calculated for three sets of parameters used in this study is presented in Fig. 1, which shows clearly that the adopted approximation represents the main features of the real interaction energy: the presence of both repulsion and attraction as well as the presence of a potential well. Changing parameters allows changing not only the depth of potential well but also the shape of potential curve – the range of colloidal forces and co-ordinate, where the energy has a minimum. Actually, if a precise potential curve, based, for example, on Eqs. (2)–(9) and accounting for the retardation effect is known then it can be fitted by using the accepted model with a reasonable accuracy.

It has been assumed that the density difference between particles and dispersion medium is negligible, and therefore pure perikinetic aggregation is considered. It was also assumed the presence of strong repulsion barrier preventing the coagulation in the deep primary minimum.

Eq (14) was solved for the particles with radius 1 μm by the finite difference Euler's method taking into account the interaction of a particle with nearest neighbours. Periodic boundary conditions were imposed on the whole system to simulate the behaviour of an unbounded colloidal suspension. A uniform initial distribution of particles over the 2-D lattice was used. The set of Langevin equation with the inertial term included was used in simulations. In this case the average velocity of particle corresponds to its energy of thermal motion [69,70] and in this way is an important control parameter assuring that there is no artificial pumping or loss of energy. The initial particles velocities, V_i, were generated according to the Maxwell distribution.
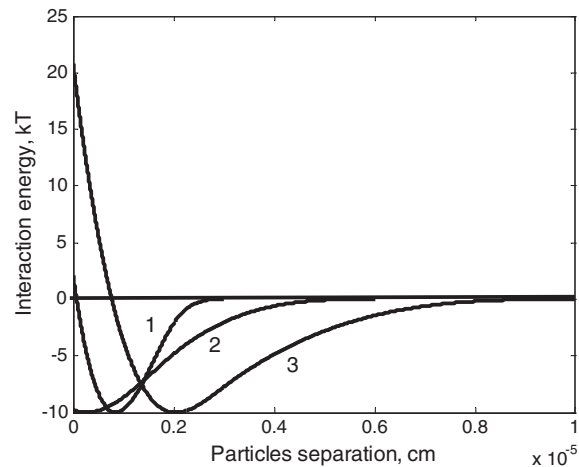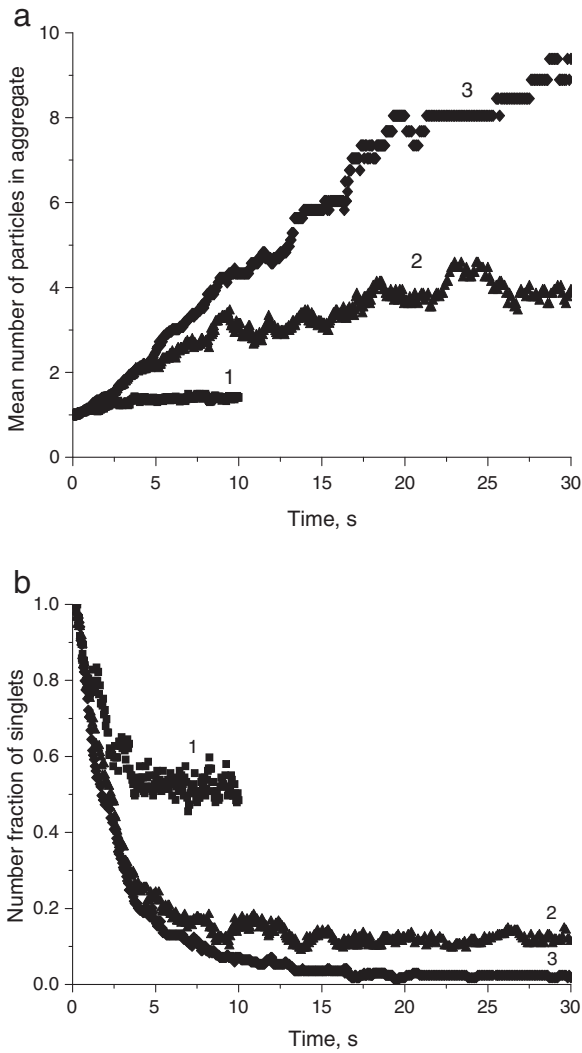

Fig. 1. Energy of interaction between particles used in the numerical simulations: $U_{min} = 10$ kT, $1 - h_1 = 1.6 \cdot 10^{-6}$ cm, $h_0 = 2.0 \cdot 10^{-6}$ cm, $h_2 = 3.0 \cdot 10^{-6}$ cm; $2 - h_1 = 1.6 \cdot 10^{-6}$ cm, $h_0 = 2.0 \cdot 10^{-6}$ cm, $h_2 = 6.0 \cdot 10^{-6}$ cm; $3 - h_1 = 2.9 \cdot 10^{-6}$ cm, $h_0 = 3.0 \cdot 10^{-6}$ cm, $h_2 = 10.0 \cdot 10^{-6}$ cm.
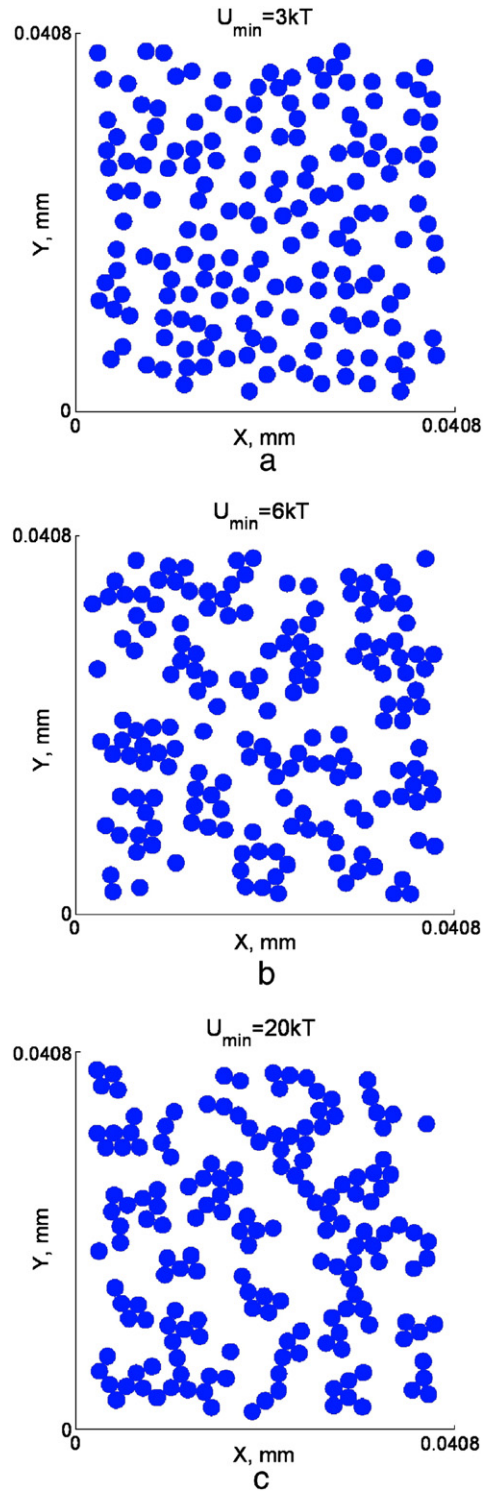
Fig. 2. Dependence of aggregation kinetics on the depth of potential well: $h_1 = 1.6 \cdot 10^{-6}$ cm, $h_0 = 2.0 \cdot 10^{-6}$ cm, $h_2 = 10.0 \cdot 10^{-6}$ cm; fraction of solid 0.32; 1 – $U_{min} = 3$ kT; 2 – $U_{min} = 6$ kT; 3 – $U_{min} = 20$ kT.

4. Results and discussions

Fig. 2 demonstrates dependency of aggregation kinetics on the depth of potential well. Two parameters have been calculated, which are the average number of particles in the aggregate (Fig. 2a) and the number fraction of singlets (Fig. 2b). It can be seen that the equilibrium establishes very quickly at the small depth of the potential well, which is now 3 kT. As the interaction energy in this case is close to the energy of the thermal motion, the long living clusters are absent at 3 kT and mainly doublets and triplets with the short life time appear as it is seen in Fig. 3a. Only about 50% of particles are included in these temporary small aggregates which are in the dynamic equilibrium with singlets.
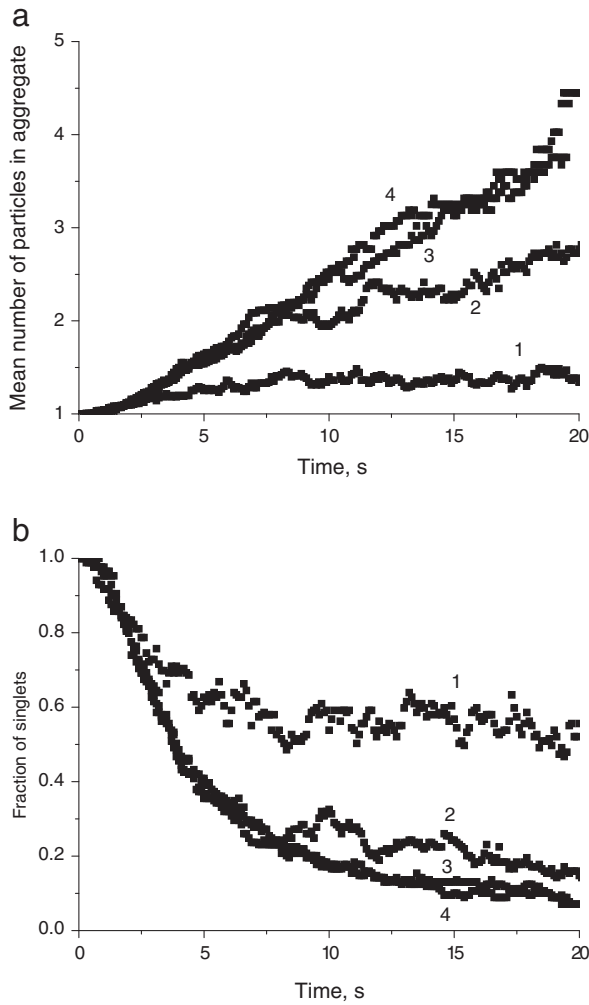
By the increase of the depth of potential well the growth rate of aggregates increases and the decrease of singlets occurs more quickly, but time needed to equilibrate the system increases. Aggregates size increases with the increase of the interaction energy, whereas the number of singlets decreases. At $U_{min} = 6$ kT the average number of particles in the aggregate reaches about 3.5, there are already rather large long-living aggregate in dynamic equilibrium with singlets (Fig. 3b). The number fraction of singlets is about 15%. At $U_{min} = 20$ kT one can expect irreversible aggregation in the system and indeed, the singlets practically disappears in this case already after 20 s (Fig. 2b,

Fig. 3. Aggregates formed at the various depths of potential well: $h_1 = 1.6 \cdot 10^{-6}$ cm, $h_0 = 2.0 \cdot 10^{-6}$ cm, $h_2 = 10.0 \cdot 10^{-6}$ cm; fraction of solid 0.32; time of aggregation 20 s; a – $U_{min} = 3$ kT; b – $U_{min} = 6$ kT; c – $U_{min} = 20$ kT.

curve3, Fig. 3c), the mean cluster size increases continuously and most probably in the final state all particles will belong to the one large aggregate.

In Fig. 4 the kinetic curves are presented for the shorter than in Fig. 2 range of colloidal forces and 4 different values of potential well depth. The aggregation at $U_{min} = 4$ kT is very low and more than 50% particles are singlets. It is seen that curves for $U_{min} = 8$ kT and

Fig. 4. Dependence of aggregation kinetics on the depth of potential well: $h_1 = 1.6 \cdot 10^{-6}$ cm, $h_0 = 2.0 \cdot 10^{-6}$ cm, $h_2 = 6.0 \cdot 10^{-6}$ cm; fraction of solid 0.32; 1 – $U_{min} = 4$kT; 2 – $U_{min} = 6$ kT; 3 – $U_{min} = 8$ kT; 4 – $U_{min} = 20$ kT.
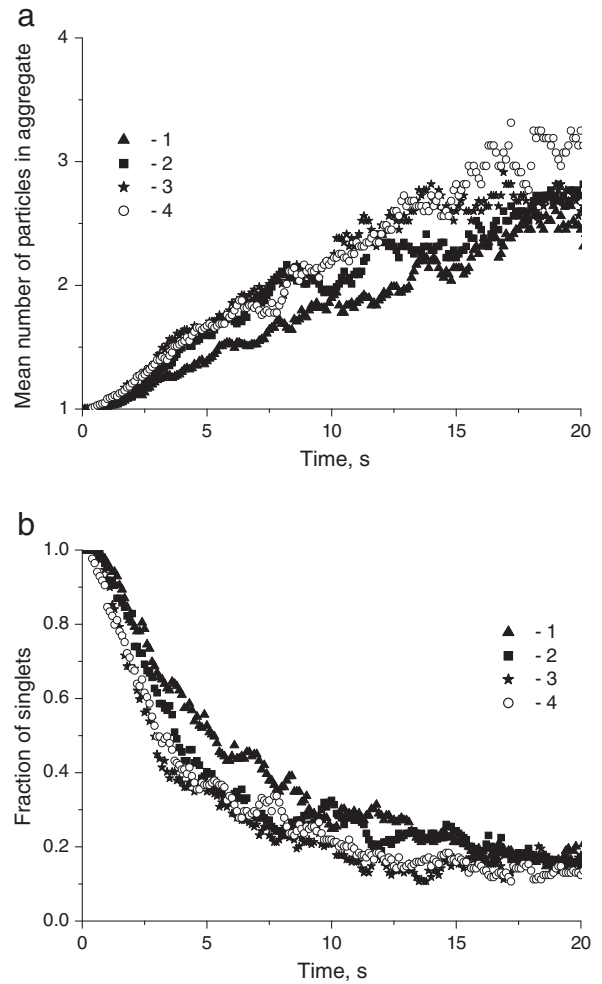

Fig. 5. Dependence of aggregation kinetics on the shape of potential well: $U_{min} = 6$ kT; fraction of solid 0.26; 1 $- h_1 = 1.6 \cdot 10^{-6}$ cm, $h_0 = 2.0 \cdot 10^{-6}$ cm, $h_2 = 3.0 \cdot 10^{-6}$ cm; 2 $- h_1 = 1.6 \cdot 10^{-6}$ cm, $h_0 = 2.0 \cdot 10^{-6}$ cm, $h_2 = 6.0 \cdot 10^{-6}$ cm; 3 $- h_1 = 1.6 \cdot 10^{-6}$ cm, $h_0 = 2.0 \cdot 10^{-6}$ cm, $h_2 = 10.0 \cdot 10^{-6}$ cm; 4 $- h_1 = 2.9 \cdot 10^{-6}$ cm, $h_0 = 3.0 \cdot 10^{-6}$ cm, $h_2 = 10.0 \cdot 10^{-6}$ cm.

$U_{min} = 20$kT are very close to each other and show practically linear increase of the mean number of particles in the aggregate n_c with time t. It is in line with the Smoluchovski theory, which predicts

$$n_c = 1 + k_F n_0 t, \tag{28}$$

where k_F is the flocculation rate constant, n_0 is the initial number concentration of particles. At the same time the shape of aggregates obtained for the case of irreversible aggregation (Fig. 3b) is far from spherical supposed by Smoluchovski. The interval of the interaction energies where the formation of stable clusters in equilibrium with singlets can be expected is between 4 and 8 kT, at least for the chosen range of colloidal forces.

Noteworthy that the results presented in Figs. 2 and 4 are in a good qualitative agreement with the experimental data on formation of equilibrium aggregates, namely on the time dependence of the reciprocal of the number concentration of particles, which characterizes the size of aggregates (Ref. [74], Fig. 1), and time dependence of percentage of singlets in suspension (Ref. [75], Fig. 2).

Surprisingly the range of colloidal forces affects only slightly the aggregation process (Fig. 5). The general trend is, as it could be expected, the decrease of range of colloidal forces slows down the aggregation, decreases the aggregates size and increases the number

fraction of singlets. This trend is seen more clearly at larger volume fractions.

The decrease of fraction of solid results in the deceleration of aggregation for all studied parameters of potential well. Remarkably, that even in the case of irreversible aggregation ($U_{min} = 20$ kT) at fraction of solid 0.19 there still remain about 10% singlets after 30 s of aggregation (Fig. 6). At $U_{min} = 6$ kT and the same values of h_0, h_1 and h_2 as in Fig. 6, by the decrease of fraction of solid from 0.32 to 0.19 the number fraction of singlets increases from about 15% to about 30% and the mean number of particles in aggregate decreases from about 3.5 to 2 after 30 s of aggregation.
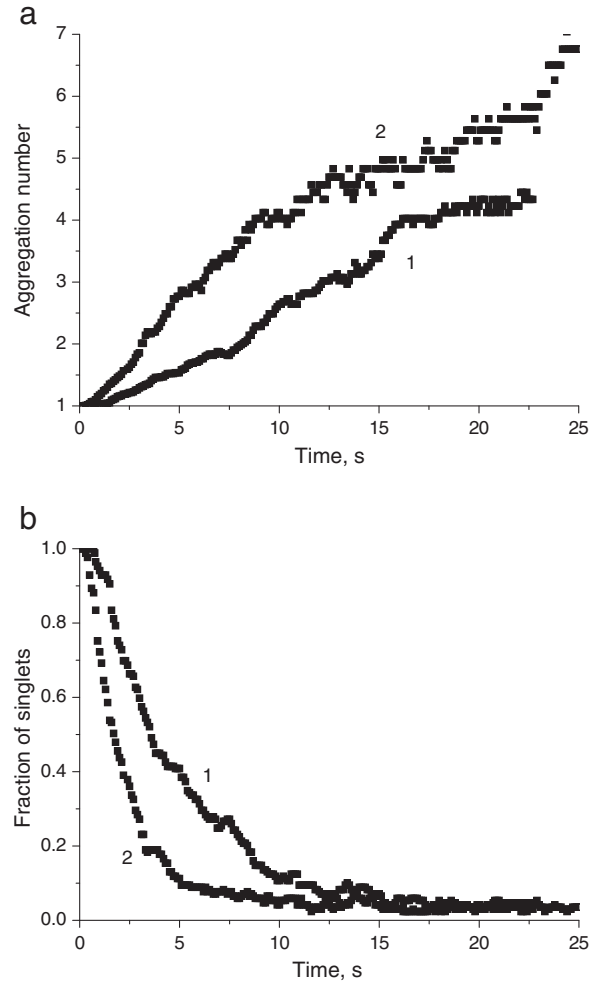
The importance of hydrodynamic interactions between particles is clear from Fig. 7. The hydrodynamic resistance to the particles approaches increases greatly as the separation decreases (see Eqs. (18) and (19)). That means that the particles move slower under action of the same force at shorter distances. The hydrodynamic interactions slows down the aggregation processes and, if they are not taken into account, then the time of the system equilibration is underestimated, whereas the mean cluster size is overestimated. This tendency was clearly seen for all studied parameters of potential well and fraction of solid. As the considered here case is two-dimensional, it may be not quite correct to compare the values of flocculation rate
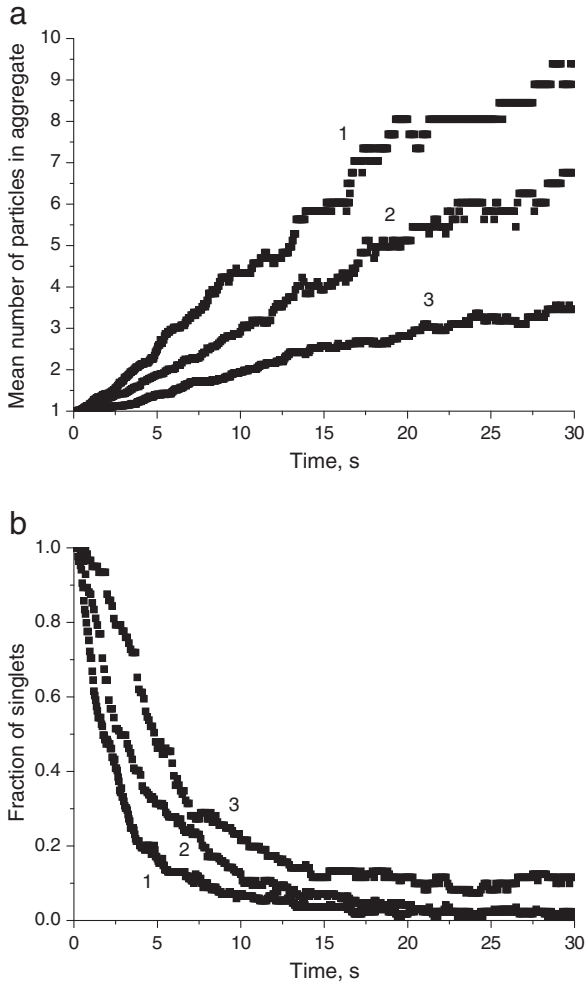
Fig. 6. Dependence of aggregation kinetics on the fraction of solid: $h_1 = 1.6 \cdot 10^{-6}$ cm, $h_0 = 2.0 \cdot 10^{-6}$ cm, $h_2 = 10.0 \cdot 10^{-6}$ cm; $U_{min} = 20$ kT; fraction of solid: 1 – 0.32; 2 – 0.26; 3 – 0.19.

Fig. 7. Dependence of aggregation kinetics on hydrodynamic interactions: $h_1 = 1.6 \cdot 10^{-6}$ cm, $h_0 = 2.0 \cdot 10^{-6}$ cm, $h_2 = 3.0 \cdot 10^{-6}$ cm; $U_{min} = 20$ kT; fraction of solid 0.26: 1 – with hydrodynamic interactions, 2 – without hydrodynamic interactions.

constant with those obtained from Smoluchovski theory, namely $k_F = 6.1 \cdot 10^{-18}$ m³/s for the case when hydrodynamic interactions and colloid forces are not taken into account [52]. Nevertheless extrapolation of the results presented in Fig. 7a to three-dimensional conditions gives the values $k_F = 8.2 \cdot 10^{-18}$ m³/s for the case when hydrodynamic interactions are not taken into account and $k_F = 4.9 \cdot 10^{-18}$ m³/s when they do. So, the agreement is surprisingly good. The higher in comparison to Smoluchovski theory value for k_F obtained in numerical simulations in absence of hydrodynamic interactions is obviously the result of acceleration of aggregation due to colloidal attraction. It is also easy to calculate, that the rate constant becomes of about 1.7 times smaller, when hydrodynamic interactions are taken into account. Characteristic flocculation time, i.e. the average time between collisions of particles can be also estimated as about $t_f = 4$ s in the absence of hydrodynamic interactions and $t_f = 6$ s with hydrodynamic interactions for fraction of solid 0.32.

Comparison of the characteristic aggregation time with the average life time of doublets estimated in [70] enables to make some conclusions about aggregation character. The life time of doublet in potential well of depth $U_{min} = 3$ kT is about $t_d = 0.65$ s what is nearly an order of magnitude smaller than flocculation time. According to [52], if $t_d \ll t_f$ then the equilibrium state represents the equilibrium between singlets and doublets with the normalized number concentration of doublets

$$n_2 = \frac{t_d}{t_f}(1 - \exp(-t / t_d)), \tag{29}$$

The presented above numerical results are in good qualitative agreement with this conclusion. For $U_{min} = 3$ kT the time t_d is essentially lover than, but still comparable with $t_f = 6$ s, that is why not only doublets, but also a small amount of triplets are present in equilibrium state (Fig. 3a). For the system presented in Fig. 2 at equilibrium $n_1 = 0.52$, $n_2 = 0.167$, $n_3 = 0.049$. The obtained equilibrium value of n_2 is slightly larger than that calculated according to Eq. (29) ($n_2 = 0.11$), as it has been expected.

The life time of doublet in potential well of depth $U_{min} = 5$ kT is about $t_d = 4$ s, for $U_{min} = 7$ kT $t_d = 14$ s. Therefore for these cases one can expect reversible aggregation with large aggregates present and $U_{min} = 7$kT should be close to the limit of irreversible aggregation. This conclusion is also in good agreement with simulation results.

It is noteworthy, that the hydrodynamic resistance in the center-to-center direction, Eq. (18), is much larger than that in the perpendicular direction, Eq. (19). There is already no component of colloidal force in the tangential direction. Therefore, the particles

mobility in the tangential direction is much higher, resulting in the rearrangement of particles inside an aggregate, doing it more compact.

5. Conclusions

The forces acting in colloidal suspensions and affecting their stability and aggregation kinetics are considered. The approximations used for these forces in numerical simulations and the importance of the balanced account for both colloidal forces and hydrodynamic interactions are discussed. The results of numerical simulations of aggregation kinetics are discussed and compared with well known analytical approximations.

The direct numerical simulation of aggregation kinetics was performed using the mathematical model based on the Langevin equations and pairwise interaction between Brownian particles. The study has shown, that the most considerable changes in the aggregation kinetics occur at the depth of potential well between 4 and 8 kT. Just in this interval the formation of stable aggregates in dynamic equilibrium with singlets due to reversible aggregation in the shallow secondary potential well can be expected.

The kinetics of aggregation and the size of equilibrium aggregates depend on the fraction of solid. Kinetics slows down, aggregates become smaller and fraction of singlets increases by the decrease of the fraction of solid. The range of colloidal forces in the studied interval 30–100 nm does not affect essentially the aggregation kinetics, but the general trend is –the decrease of the range of colloidal forces slows down the aggregation, decreases the aggregates size and increases the number fraction of singlets.

The simulations has confirmed the importance of taking into account the hydrodynamic interactions between particles, as neglecting of these interactions result in the overestimating of aggregates growth rate.

Acknowledgements

References

[1] Deryaguin BV, Churaev NV, Muller VM. Surface forces, Consultants Bureau. New York: Plenum Press; 1987.
[2] Israelachvili JN. Intermolecular and surface forces. London: Academic Press; 1992.
[3] Cosgrove T, editor. Colloid science. Principles, methods and applications. Oxford: Blackwell; 2005.
[4] Burns JL, de Yan Y, Jameson GJ, Biggs S. Langmuir 1997;13:6413.
[5] Filippov AV, Zurita M, Rosner DE. J Coll Int Sci 2000;229:261.
[6] Bushell GS, Yan YD, Woodfield D, Raper J, Amal R. Adv Coll Int Sci 2002;95:1.
[7] Lin MY, Lindsay HM, Weitz DA, Klein R, Ball RC, Meakin P. J Phys Condens Matter 1990;2:3093.
[8] Lin MY, Lindsay HM, Weitz DA, Ball RC, Klein R, Meakin P. Phys Rev A 1990;41: 2005.
[9] Long JA, Osmond DWJ, Vincent B. J Coll Int Sci 1973;42:545.
[10] Muller VM. Colloid J 1996;58:598.
[11] Urbina-Villalba G, Garcia-Sucre M. Langmuir 2005;21:6675.
[12] Groenewold J, Kegel WK. J Phys Chem B 2001;105:11702.
[13] Sciortino F, Mossa S, Zaccareli E, Tartaglia P. Phys Rev Lett 2004;93:055701.
[14] Mossa S, Sciortino F, Tartaglia P, Zaccareli E. Langmuir 2004;20:10756.
[15] Piazza R, Pierno M, Iacopini S, Mangione P, Esposito G, Belotti V. Eur Biophys J 2006;35:439.
[16] Jeffrey GC, Ottewill RH. Colloid Polym Sci 1990;268:179.
[17] Golikova EV, Chernoberezhskii YuM, Ioganson OM, Vysokovskaya NA, Grigor'ev VS. Coll J 2003;65(N4):420.
[18] Segre PN, Prasad V, Schofield AB, Weitz DA. Phys Rev Lett 2001;86:6042.
[19] Dinsmore AD, Weitz DA. J Phys Condens Matter 2002;14:7581.
[20] Sedgwick H, Egelhaaf SU, Poon WCK. J Phys Condens Matter 2004;16:S4913.
[21] Stradner A, Sedgwick H, Cardinaux F, Poon WCK. Nature 2004;432:492.
[22] Campbell AI, Anderson VJ, van Duijneveldt JS, Bartlett P. Phys Rev Lett 2005;94: 208301.
[23] Sanchez R, Bartlett P. J Phys Condens Matter 2005;17:S3551.
[24] Quemada D, Berli C. Adv Coll Int Sci 2002;98:51.
[25] Friend JP, Hunter RJ. J Coll Int Sci 1971;37:548.
[26] Starov V, Zhdanov V, Meireles M, Molle C. Adv Coll Int Sci 2002;96:279.
[27] Starov VM, Zhdanov VG. Adv Coll Int Sci 2008;137:2.
[28] Kovalchuk NM, Kuchin I, Starov V, Uriev N. Coll J 2010;72(N3):379.
[29] Kovalchuk N, Starov V, Holdich R. Coll J 2010;N5:1.
[30] Haw MD, Sievwright M, Poon WCK, Pusey PN. Adv Coll Int Sci 1995;62:1.
[31] Imperio A, Reatto L. J Phys Condens Matter 2004;16:S3769.
[32] Charbonneau P, Reichman DR. Phys Rev E 2007;75:011507.
[33] Delhommelle J, Petravic J. J Chem Phys 2005;123:074707.
[34] Espanol P. Phys Rev E 1995;52:1734.
[35] Odrizola G, Schmitt A, Moncho-Jorda A, Callejas-Fernandez J, Martinez-Garcia R, Leone R, et al. Phys Rev E 2002;65:031405.
[36] Selomulya C, Bushell G, Amal R, Waite TD. Chem Eng Sci 2003;58:327.
[37] Odrizola G, Leone R, Schmitt A, Callejas-Fernandez J, Martinez-Garcia R, Hidalgo-Alvarez R. J Chem Phys 2004;121:5468.
[38] Kim JW, Kramer NA. Coll Surf A 2005;253:33.
[39] Ermak DL, McCammon JA. J Chem Phys 1978;69:1352.
[40] Ansell GC, Dickinson E, Ludvigsen M. J Chem Soc Faraday Trans 1985;2(81):1269.
[41] Bossis G, Brady JF. J Chem Phys 1987;87:5437.
[42] Branka AC, Heyes DM. Phys Rev E 1999;60:2381.
[43] Albers J, Deutsch JM, Oppenheim I. J Chem Phys 1971;54:3541.
[44] Deutsch JM, Oppenheim I. J Chem Phys 1971;54:3547.
[45] Deutch JM, Oppenheim I. Faraday Discuss Chem Soc 1987;83:1.
[46] Coffey WT, Kalmykov YuP, Waldron JT. The Langevin equation. With applications in physics, chemistry and electrical engineering. World scientific series in contemporary chemical physics, 11. World scientific publishing; 1996.
[47] Elimeleh M, Gregory J, Jia X, Williams RA. Particle Deposition and Aggregation. Oxford: Butterworth-Hanemann; 1995.
[48] Chen JC, Kim AS. Adv Coll Int Sci 2004;112:159.
[49] Spielman LA. J Coll Int Sci 1970;33:439.
[50] Dickinson E. J Coll Int Sci 1984;98:587.
[51] Ansell GC, Dickinson E. Chem Phys Let 1985;122:595.
[52] Dukhin SS, Sjoblom J, Saether Q. An Experimental and Theoretical Approach to Dynamic Behavior of Emulsians. In: Sjoblom J, editor. Emulsion and Emulsion Stability. second. London: Taylor and Frances; 2006.
[53] Rabinovich YaI, Chuaev NV. Coll J 1990;52(N2):309.
[54] Jenkins P, Snowden M. Adv Coll Int Sci 1996;68:57.
[55] Genovese DB, Lozano JE. Food Hydrocolloids 2006;20:767.
[56] Dukhin AS, Dukhin SS, Goetz PJ. Adv Coll Int Sci 2007;134–135:35.
[57] Muller VM. Coll J 1978;40:735.
[58] Dukhin SS, Mishchuk NA, Loglio G, Liggien L, Miller R. Adv Coll Int Sci 2003;100– 102:47.
[59] Sullivan F, Mountain RD. Comp Phys Com 1986;42:43.
[60] Uriev NB, Cheremisov AV, Tkachev AYu. Coll J 1999;61:413.
[61] Uriev NB, Kuchin IV, Naumenko EA. Coll J 2007;69(N6):792.
[62] Derjaguin BV, Muller VM. Dokl Akad Nauk SSSR 1967;176:738.
[63] Honig EP, Roebersen GJ, Wiershema PH. J Coll Int Sci 1971;38:97.
[64] Batchelor GK. J Fluid Mech 1976;74:1.
[65] Foss DR, Drady JF. J Rheol 2000;44(3):629.
[66] Cordelair J, Greil P. J Europ Ceram Soc 2004;24:2717.
[67] Bacon J, Dickinson E, Parker R. J Chem Soc Faraday Trans 1983;2(79):91.
[68] Ball RC, Melrose JR. Physica A 1997;247:444.
[69] Kovalchuk N, Starov V, Langston P, Hilal N. J Coll Int Sci 2008;325:377.
[70] Kovalchuk N, Starov V, Langston P, Hilal N. Coll J 2009;71:503.
[71] Cox RG. Int J Multiphase Flow 1974;1:343.
[72] Turq P, Lanteime F, Friedman HL. J Chem Phys 1977;66:3039.
[73] Groot RD, Warren PB. J Chem Phys 1997;107:4423.
[74] Golikova EV, Chernoberezhskii YuM, Grigor'ev VS, Semenov MP. Glass Phys Chem 2006;32:646.
[75] Cornell RM, Goodwin JW, Ottewill RH. J Coll Int Sci 1979;71:254.